



PII: S1386-1425(19)30799-1  
 DOI: <https://doi.org/10.1016/j.saa.2019.117409>  
 Article  
 Number: 117409  
 Reference: SAA 117409

Received date: 15 February 2019  
Revised date: 19 July 2019  
Accepted date: 20 July 2019

This is a PDF file of an unedited manuscript that has been accepted for publication. As a service to our customers we are providing this early version of the manuscript. The manuscript will undergo copyediting, typesetting, and review of the resulting proof before it is published in its final form. Please note that during the production process errors may be discovered which could affect the content, and all legal disclaimers that apply to the journal pertain.

**Title:** Rational design of a colorimetric and fluorescence turn-on chemosensor with benzothiazolium moiety for cyanide detection in aqueous solution

**Author names and affiliations:**

Name	Country	Affiliations	E-mail
Beibei Zhai	China	Wuhan Textile University, Wuhan 430073, Hubei, PR China	1379962526@qq.com
Ziwei Hu	China	Wuhan Textile University, Wuhan 430073, Hubei, PR China	771704605@qq.com
Chun Peng	China	Wuhan Textile University, Wuhan 430073, Hubei, PR China	374397673@qq.com
Bing Liu	China	Wuhan Textile University, Wuhan 430073, Hubei, PR China	1520352351@qq.com
Wei Li	China	Wuhan Textile University, Wuhan 430073, Hubei, PR China	liwei_w hu@sohu.com
Chao Gao	China	Wuhan Textile University, Wuhan 430073, Hubei, PR China	chgao@wtu.edu.cn

**Corresponding author:**

Name: Chao Gao; Email: chgao@wtu.edu.cn

**Permanent address of the corresponding author:**

Hubei Key Laboratory of Biomass Fibers and Eco-dyeing & Finishing, department of Chemistry and Chemical Engineering, Wuhan Textile University, Yangguang Avenue, Wuhan 430073, Hubei, PR China.

**Abstract:** A novel colorimetric and fluorescence turn-on chemosensor **TBB** with benzothiazolium moiety has been explored, which exhibited the high selectivity for cyanide ion ( $\text{CN}^-$ ) in THF– $\text{H}_2\text{O}$  (2:8, v/v) mixture. The aqueous solution of sensor **TBB** was scarcely emissive. In the presence of  $\text{CN}^-$  ion, the nucleophilic addition of  $\text{CN}^-$  with the benzothiazolium C=N bond of **TBB** produced the new species **TBB–CN**, consequently resulting in the intense orange–red emission by aggregation-induced emission (AIE) effect. Meanwhile, the color of solution was changed from orange-yellow to light yellow. The sensing mechanism was verified by Mass spectrometry, NMR analysis and DFT calculations.

**Keywords:** Benzothiazolium; Cyanide ion; Chemosensor; Aggregation-induced emission.

## 1. Introduction

Cyanide salts, as a kind of extremely useful materials, have been widely utilized in many fields including the electroplating, metallurgy, tanning and plastics production [1-3]. But cyanide ion ( $\text{CN}^-$ ) was highly toxic to mammals, because it could impede the oxidative metabolism process, destroy the mitochondrial electron transport chain and injure the central nervous system. Furthermore, it directly caused the death of human at the concentration of 0.7–3.5 mg/kg of body weight [4,5]. In accordance with the World Health Organization (WHO), the concentration of  $\text{CN}^-$  ion in drinking water should be less than 1.9  $\mu\text{M}$  [6]. Therefore, the development of a simple and efficient method for

monitoring the concentration of  $\text{CN}^-$  ion in environmental and biological systems was particularly significant.

Among the various detection technologies for  $\text{CN}^-$  ion, fluorescence analysis has attracted more attentions owing to the advantages of low cost, convenient use and simple preparation. So far, a plenty of fluorescent chemosensors with various mechanisms for  $\text{CN}^-$  ion detection have been reported [7,8]. It was well known that  $\text{CN}^-$  ion was an excellent nucleophile, and the sensors based on the nucleophilic addition reaction commonly displayed the high selectivity to  $\text{CN}^-$  ion. Comparing with the carbonyl groups and electron-deficient alkenes, the benzothiazolium  $\text{C}=\text{N}$  group was easier attacked by the nucleophilic  $\text{CN}^-$  ion, which endowed the benzothiazolium-based sensors with the faster response toward  $\text{CN}^-$  ion [9]. In addition, these sensors could detect  $\text{CN}^-$  ion directly by naked-eyes due to the color change. In spite of this, they were still confronted with the problems. Firstly, some of them exhibited the fluorescence turn-off response, because the nucleophilic addition reaction of  $\text{CN}^-$  ion with the benzothiazolium moiety interrupted the conjugation of sensors, and blocked the Intramolecular Charge Transfer (ICT) processes, consequently resulting in the fluorescence quenching [9–12]. The “turn off” sensors were regarded as unreliable because many other factors could cause fluorescence quenching [13,14]. Then, the other sensors were based on the pyrene-benzothiazolium,

naphthopyran-benzothiazolium or naphthalimide-benzothiazolium conjugates. The detection of  $\text{CN}^-$  ion was generally conducted in the aqueous solutions with 50% volume fraction of volatile and toxic organic solvents [15–17]. Notably, the above shortcomings significantly restricted their practical application in  $\text{CN}^-$  ion sensing.

Aggregation-induced emission (AIE) effect was widely used in the design of fluorescence “turn on” chemosensors [18–20]. The D–A type triphenylamine–benzothiadiazole conjugates exhibited the long wavelength emission owing to the push-pull electron process. In which, the triphenylamine (TPA) group served as the electron donor (D), and the benzothiadiazole (BT) unit was the electron acceptor (A). In addition, these conjugates generally possessed the combined twist-intramolecular charge transfer (TICT) and AIE effects, that the emission intensity was decreased along with the increase of solvent polarity, but enhanced in the aggregate state [21]. The cationic benzothiazolium moiety was hydrophilic, and its introduction into the TPA–BT based luminophors could improve the water solubility. These new constructed luminophors were scarcely or non emissive in high polar solvents. In the presence of  $\text{CN}^-$  ion, its nucleophilic addition reaction to benzothiazolium moiety destroyed the cationic structure and decreased the water-solubility of these luminophors. Consequently, the aggregation of new additive species resulted in the intense emission by AIE mechanism.

Herein, a novel triphenylamine–benzothiadiazole based sensor **TBB** for  $\text{CN}^-$  ion has been developed, which utilized the benzothiazolium moiety as the recognition group. Sensor **TBB** was barely emissive in the THF– $\text{H}_2\text{O}$  (2:8, v/v) mixture. On treatment with  $\text{CN}^-$  ions, the solution exhibited the intense orange–red emission by AIE effect, and its color was changed from orange-yellow to light yellow. Comparing with other similar works, sensor **TBB** possessed the several advantages (Table S1). Firstly, **TBB** displayed the fluorescence turn-on response toward  $\text{CN}^-$  ion. Secondly, the detection medium contained small amount of organic solvent (20 vol %). Thirdly, the detection limit of **TBB** to  $\text{CN}^-$  ion (137 nM) was lower than most other benzothiazolium-based sensors and the WHO guideline (1.9  $\mu\text{M}$ ). Finally, the response time of 3 min was far shorter than some other similar sensors.

## 2. Experimental section

### 2.1. Materials and Instruments

Unless the otherwise stated, the reagents and solvents were purchased from Energy Chemical (China) CO., Ltd with the guarantee reagent (GR) grade, and they were used directly without the further purifications. 4-Bromo-7-[4-(diphenylamino)phenyl]-2,1,3-benzothiadiazole and 3-ethyl-2-methylbenzo[d]thiazol-3-ium bromide were obtained according to the reported methods [22,23]. The synthetic procedure of compound **1**

was described in the supporting information. Double distilled water was used in all the experiments. NMR spectra were obtained on the Bruker Ascend 400 MHz Nuclear Magnetic Resonance Spectrometer. The  $^1\text{H}$  NMR (400 MHz) chemical shifts were given using  $\text{CDCl}_3$  as the internal reference ( $\text{CDCl}_3$ :  $\delta = 7.26$  ppm). The  $^{13}\text{C}$  NMR (100 MHz) chemical shifts were recorded using  $\text{CDCl}_3$  as the internal standard ( $\text{CDCl}_3$ :  $\delta = 77.16$  ppm). High-resolution mass spectra (HRMS) were taken on with a Bruker-Q-TOF mass spectrometer. Melting points were measured with SGW X-4 instrument. Absorption spectra were tested on TU-1901 spectrometer. The fluorescence spectra were got with the HITACHI F-2500 fluorescence spectrometer. The pH measurements were prepared by Sartorius PB-10 meter. Dynamic light scattering (DLS) experiments were investigated with Malvern ZS90 particle sizer.

## 2.2. Synthesis of sensor **TBB**

A mixture of compound **1** (242 mg, 0.5 mmol) and 3-ethyl-2-methylbenzo[d]thiazol-3-ium bromide (154 mg, 0.6 mmol) in EtOH (4 mL) was refluxed overnight under  $\text{N}_2$ . After that, the mixture was concentrated using rotavapor, and the residue was purified by a silica gel column ( $\text{DCM}/\text{MeOH} = 6/1$ , v/v) to provide **TBB** as a claret red solid (191 mg, yield: 53%). m.p. 214.6-216.2 °C.  $^1\text{H}$  NMR (400 MHz,  $\text{CDCl}_3$ ):  $\delta$  (ppm) 8.47 (d,  $J = 15.6$  Hz, 1H, vinyl H), 8.26-8.27 (m, 2H, -ArH), 8.17

(d,  $J = 15.6$  Hz, 1H, vinyl H), 8.04 (d,  $J = 7.6$  Hz, 2H, -ArH), 7.88 (d,  $J = 8.4$  Hz, 2H, -ArH), 7.72-7.76 (m, 3H, -ArH), 7.47-7.55 (m, 3H, -ArH), 7.29-7.33 (m, 4H, -ArH), 7.18-7.22 (m, 2H, -ArH), 7.09 (t,  $J = 7.4$  Hz, 2H, -ArH), 5.32-5.39 (m, 2H, -CH<sub>2</sub>), 1.51 (t,  $J = 7.0$  Hz, 3H, -CH<sub>3</sub>); <sup>13</sup>C NMR (100 MHz, CDCl<sub>3</sub>):  $\delta$  (ppm) 171.93, 154.27, 153.89, 148.57, 147.52, 141.59, 140.89, 134.10, 131.24, 130.51, 130.40, 130.16, 129.87, 129.76, 129.56, 128.91, 128.56, 127.20, 125.25, 125.13, 124.49, 123.69, 122.69, 115.95, 114.94, 113.50, 52.57, 14.98. HRMS (ESI<sup>+</sup>):  $m/z$  calcd. for C<sub>41</sub>H<sub>31</sub>N<sub>4</sub>S<sub>2</sub> [M-Br]<sup>+</sup> 643.1985; found 643.1987.

### 2.3. Photophysical measurements

The sodium salts of anions (F<sup>-</sup>, Cl<sup>-</sup>, Br<sup>-</sup>, I<sup>-</sup>, H<sub>2</sub>PO<sub>4</sub><sup>-</sup>, AcO<sup>-</sup>, N<sub>3</sub><sup>-</sup>, NO<sub>3</sub><sup>-</sup>, SO<sub>4</sub><sup>2-</sup> and SCN<sup>-</sup>) and the tetrabutylammonium salt of CN<sup>-</sup> were used for the UV-vis absorption spectra and fluorescence spectra measurements. The selectivity experiments of sensor **TBB** toward CN<sup>-</sup> were performed with the same concentration of various anions. About the titration experiments, different concentrations of CN<sup>-</sup> were added into the aqueous solution of **TBB**, and then measured the absorption spectra and fluorescence spectra respectively. The fluorescence intensity was recorded by fluorescence spectrometer that the slit width was kept at 10 nm.

### 2.4. The calculation of detection limit



The detection limit (DL) was calculated according to the common equation “ $DL = 3\sigma/k$ ” that the value of signal-to-noise ratio (S/N) was regulated at “3” [24]. In which, “ $\sigma$ ” was the standard deviation of blank measurements (8 times detection), and “ $k$ ” represented the slope between fluorescence intensity versus the concentration of  $CN^-$ .

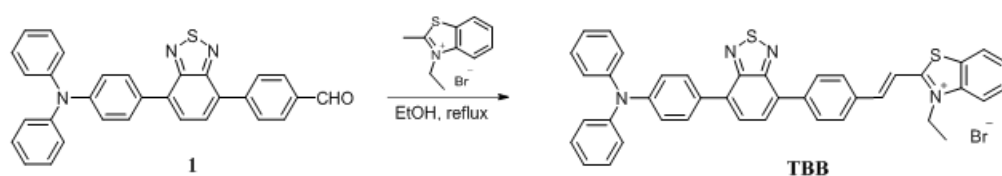
### 2.5. Theoretical calculations

All the calculations were performed with Gaussian 16 program suite. The first singlet excited states geometries were optimized by TDDFT approaches at TD-M062X level, which used  $H_2O$  as the solvent molecule. The frontier molecular orbitals and energy levels were calculated by the TD-B3LYP level.

## 3. Results and discussion

### 3.1. Synthesis and characterization

The synthetic route of sensor **TBB** was showed in Scheme 1. Briefly, the condensation reaction of compound **1** with 3-ethyl-2-methylbenzo[d]thiazol-3-ium bromide gave **TBB** with a moderate yield. The chemical structures of **TBB** were confirmed by  $^1H$  NMR,  $^{13}C$  NMR and HRMS.



**Scheme 1.** The synthetic route of sensor **TBB**

### 3.2. The fluorescence properties of sensor **TBB**

The reported TPA-BT based conjugates generally possessed the combined twisted intramolecular charge transfer (TICT) and AIE characteristics. Their emission intensity was weakened along with the increase of solvent polarity. In large polar solvents, these compounds tended to form the twisted charge-separated conformations through the intramolecular rotation, whose excited-state energy was consumed non-radioactively, consequently leading to the weak or even no emission. While in the aggregate state, the intramolecular rotation was restricted, and the highly twisted molecular conformations hampered the intermolecular  $\pi$ - $\pi$  stacking interactions. Thus, the combined effects resulted in the intense emission. Notably, the TICT process caused the weak or no emission in large polar solvents, and AIE effect was responsible for the intense emission in the aggregate state [25,26]. In view of this, the fluorescence properties of **TBB** (10  $\mu$ M) in various polar solvents were firstly studied. As shown in Fig. 1, **TBB** exhibited the extremely weak emission in all the solvents, including the low polar toluene, DCM and THF, which was distinctly different from some reported TPA-BT based derivatives [21,27,28].

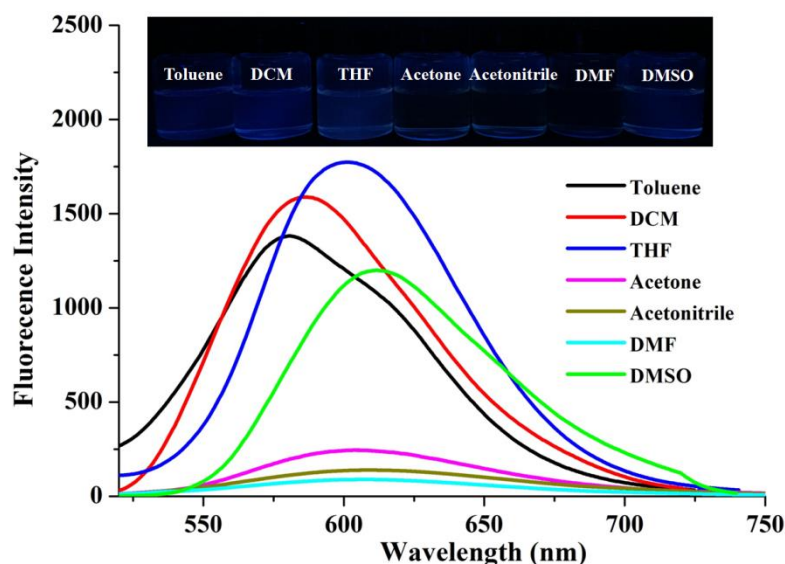


**Fig. 1.** The fluorescence spectra of sensor **TBB** (10  $\mu$ M) in different polar solvents, and the solutions were excited at their own maxima excitation. Inset: the photographs of **TBB** in various solvents were taken under 365 nm light illumination.

### 3.3. The AIE property of sensor **TBB**

Subsequently, the AIE property of sensor **TBB** (10  $\mu$ M) was investigated in THF/water mixed solutions with different volume fractions of water ( $f_w$ ). Similarly with the preceding results, **TBB** (10  $\mu$ M) was scarcely emissive in the pure THF. Upon the increase of  $f_w$ , the maximum emission peak had a slight red-shift and the fluorescence intensity exhibited a mild decrease (Fig. 2), which were caused by the improvement of solvent polarity [29]. Sensor **TBB** was able to aggregate in THF/water mixture until  $f_w$  was up to 99 vol %. The DLS results illustrated that the average size of formed nanoaggregates in this solution was around 350.7 nm (Fig. S1). But the solution still exhibited the extremely weak emission (Fig. 2). Apparently, **TBB** didn't possess the

AIE activity that exhibited the scarce emission both in dilute solution and in the aggregate state. Moreover, **TBB** displayed the faint emission in TLC plate and solid state, which further certified the non-AIE activity of **TBB** (Fig. S2). When the anion of **TBB** was exchanged to be tetrafluoroborate ion ( $\text{BF}_4^-$ ), the obtained solid was also scarcely emissive (Fig. S2b), thus the scarce emission of **TBB** was not caused by the heavy atom effect of  $\text{Br}^-$  [28]. In sensor **TBB**, the BT unit and benzothiazolium moiety both showed the strong electron-withdrawing ability, which would cause the intense intramolecular charge transfer and dipole-dipole interactions, thus leading to the emission quenching in essence [30].

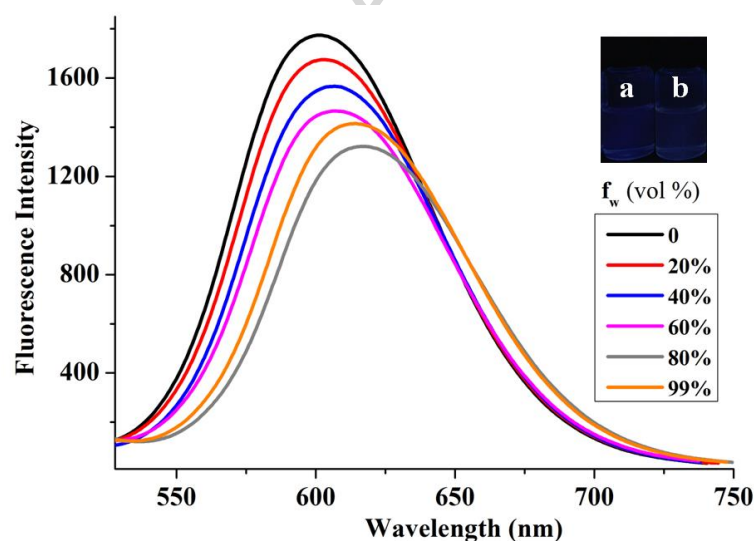


**Fig. 2.** The fluorescence spectra of sensor **TBB** (10  $\mu\text{M}$ ) in THF/water mixture with different volume fractions of water ( $f_w$ ). Insets: the photographs of **TBB** in THF (a) and THF/water mixture ( $f_w = 99$  vol %, b) under 365 nm light illumination.

### 3.4. Spectroscopic Studies of **TBB** toward $\text{CN}^-$

The sensing behavior of sensor **TBB** (10  $\mu\text{M}$ ) toward  $\text{CN}^-$  in THF– $\text{H}_2\text{O}$  (2:8, v/v) mixed solution was studied through the UV-vis

absorption spectra and fluorescence spectra. **TBB** was well dissolved in THF–H<sub>2</sub>O (2:8, v/v) mixture, because the solution had no signal in DLS test. As shown in Fig. 3, the aqueous solution of **TBB** exhibited two absorption peaks at 403 nm and 469 nm, respectively. The DFT calculations suggested that these two peaks were caused by the  $\pi$ – $\pi^*$  electronic transition. In the presence of CN<sup>−</sup> ion (100  $\mu$ M), the absorption peaks at 403 nm and 469 nm were disappeared, and a new peak at 431 nm *via*  $\pi$ – $\sigma^*$  electronic transition was arisen, implying that the reaction of CN<sup>−</sup> ion with **TBB** was occurred. Meanwhile, the color of solution was visibly changed from orange-yellow to light yellow. Gratifyingly, the addition of other anions (H<sub>2</sub>PO<sub>4</sub><sup>−</sup>, AcO<sup>−</sup>, F<sup>−</sup>, Cl<sup>−</sup>, Br<sup>−</sup>, I<sup>−</sup>, N<sub>3</sub><sup>−</sup>, NO<sub>3</sub><sup>−</sup>, SO<sub>4</sub><sup>2−</sup> and SCN<sup>−</sup>) caused the negligible change in absorption spectra. Therefore, sensor **TBB** was capable of detecting CN<sup>−</sup> ion by the naked-eyes.

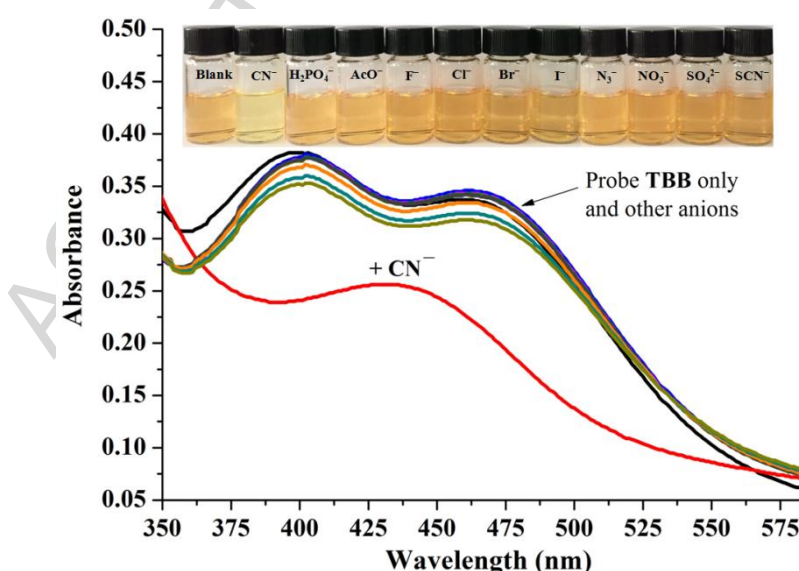


**Fig. 3.** The UV–vis absorption spectra of sensor **TBB** (10  $\mu$ M) in THF–H<sub>2</sub>O (2:8, v/v) mixed solution with the treatment of 100  $\mu$ M various anions (CN<sup>−</sup>, H<sub>2</sub>PO<sub>4</sub><sup>−</sup>, AcO<sup>−</sup>, F<sup>−</sup>, Cl<sup>−</sup>, Br<sup>−</sup>, I<sup>−</sup>, N<sub>3</sub><sup>−</sup>, NO<sub>3</sub><sup>−</sup>, SO<sub>4</sub><sup>2−</sup> and SCN<sup>−</sup>). The solutions were stirred for 3 min at 32 °C

before the measurements; Inset: The photographs of **TBB** in THF–H<sub>2</sub>O (2:8, v/v) mixed solution with various anions that taken under sunlight.

Subsequently, the fluorescence response of sensor **TBB** toward CN<sup>−</sup> ion was researched. Sensor **TBB** (10 μM) exhibited the faint emission in THF–H<sub>2</sub>O (2:8, v/v) mixture. Upon the addition of CN<sup>−</sup> ion (100 μM), an intense emission at 589 nm was emerged, and the fluorescence intensity was enhanced almost 7-fold (Fig. 4). Moreover, the DLS data indicated the aggregation of solution that the average size of nanoaggregates was around 257.9 nm (Fig. S3). Obviously, the enhancement of fluorescence intensity was caused by the AIE mechanism. The nucleophilic addition of CN<sup>−</sup> ion with **TBB** produced the new species **TBB–CN**, whose aggregation turned on the fluorescence. The addition of other anions (H<sub>2</sub>PO<sub>4</sub><sup>−</sup>, AcO<sup>−</sup>, F<sup>−</sup>, Cl<sup>−</sup>, Br<sup>−</sup>, I<sup>−</sup>, N<sub>3</sub><sup>−</sup>, NO<sub>3</sub><sup>−</sup>, SO<sub>4</sub><sup>2−</sup> and SCN<sup>−</sup>) gave a small or even no improvement of fluorescence intensity, thus **TBB** displayed the high selectivity to CN<sup>−</sup> ion.

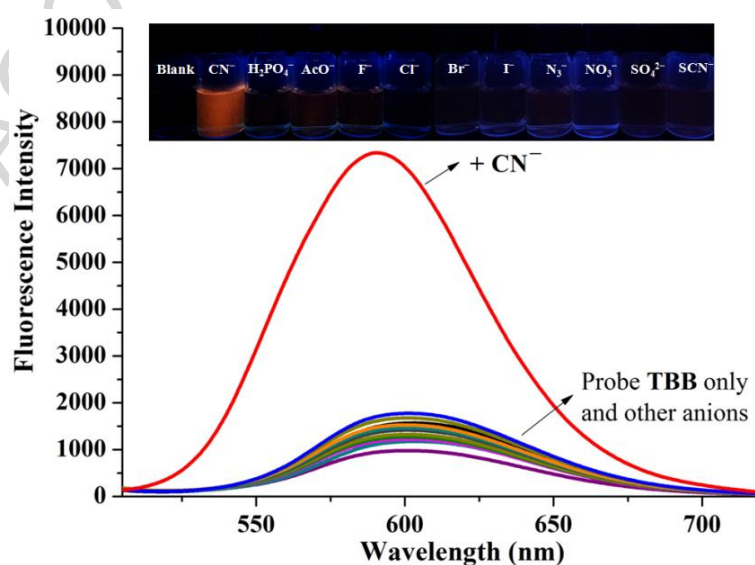


**Fig. 4.** The fluorescence spectra of sensor **TBB** (10  $\mu\text{M}$ ) in THF–H<sub>2</sub>O (2:8, v/v) mixed solution with the treatment of 100  $\mu\text{M}$  various anions ( $\text{CN}^-$ ,  $\text{H}_2\text{PO}_4^-$ ,  $\text{AcO}^-$ ,  $\text{F}^-$ ,  $\text{Cl}^-$ ,  $\text{Br}^-$ ,  $\text{I}^-$ ,  $\text{N}_3^-$ ,  $\text{NO}_3^-$ ,  $\text{SO}_4^-$  and  $\text{SCN}^-$ ), excited at 450 nm. The solutions were stirred for 3 min at 32 °C before the measurements; Inset: The photographs of **TBB** in THF–H<sub>2</sub>O (2:8, v/v) mixed solution with various anions that taken under 365 nm light.

For obtaining the detail information on the response of sensor **TBB** to  $\text{CN}^-$  ion, the titration experiments were successively performed by the absorption and fluorescence spectra. Upon the continuous addition of  $\text{CN}^-$  ion into the THF/H<sub>2</sub>O (2:8, v/v) mixed solution of **TBB** (10  $\mu\text{M}$ ), the absorbance at 403 nm and 469 nm was gradually decreased, subsequently the absorbance of new peak at 431 nm was slightly increased (Fig S4), which indicated the generation of additive species **TBB-CN**. Additionally, the addition of  $\text{CN}^-$  ion obviously enhanced the fluorescence intensity of solution. Delightfully, a great linear correlation between the fluorescence intensity at 589 nm and the concentrations of  $\text{CN}^-$  ion was observed (Fig. 5). This linear relationship was mainly caused by the increasing nanoaggregate numbers of species **TBB-CN**. According to the reported formula “ $\text{DL} = 3\sigma/k$ ”, the detection limit of (DL) sensor **TBB** toward  $\text{CN}^-$  ion was calculated to be  $1.34 \times 10^{-7}$  M, implying that **TBB** exhibited a better sensitivity toward  $\text{CN}^-$  than some other benzothiazolium-based sensors [9,10,12,15,16]. In addition, this detection limit was far lower than the safe concentration (1.9  $\mu\text{M}$ ) of WHO guideline [6], indicating

that sensor **TBB** was potentially used to monitor  $\text{CN}^-$  ion in environmental system. The Job's plot experiment illustrated the 1:1 stoichiometry for the bonding of **TBB** with  $\text{CN}^-$  ion, and this result was consistent with the other reports (Fig. S5).

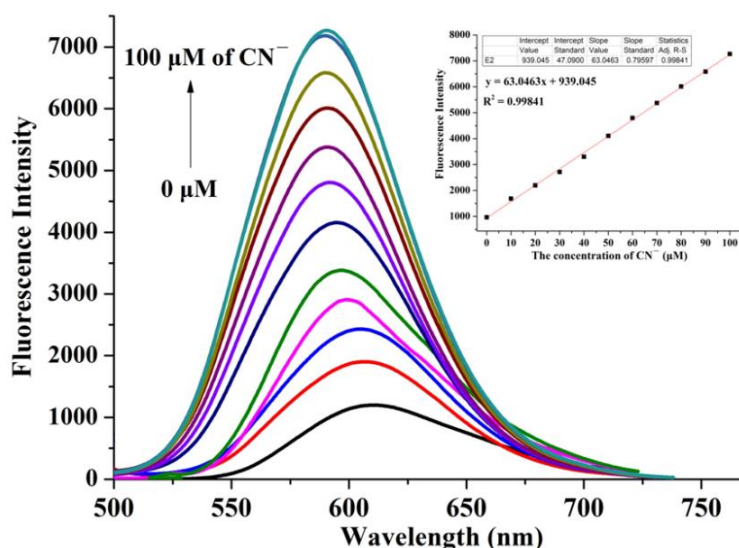


**Fig. 5.** The fluorescence spectra of sensor **TBB** (10  $\mu\text{M}$ ) in THF–H<sub>2</sub>O (2:8, v/v) mixed solution with different concentrations of  $\text{CN}^-$  ion, excited at 450 nm. The solutions were stirred for 3 min at 32 °C before the measurements; Inset: The plots of the fluorescence intensity at 589 nm *versus* the concentrations of  $\text{CN}^-$  ion. In which, the linear equation was “ $y = 63.0463x + 939.045$ ”, and  $R^2 = 0.99841$ .

After that, the time-dependent experiment of sensor **TBB** toward  $\text{CN}^-$  ion was recorded (Fig. S6). The fluorescence intensity was increased dramatically along with the time elapsing, and reached to the maximum within 3 min, implying that the reaction of  $\text{CN}^-$  ion with **TBB** was completed. This response time was distinctly shorter than some reported benzothiazolium-based sensors [9,12]. Moreover, the pH-dependent experiment of **TBB** toward  $\text{CN}^-$  ion was also studied. The fluorescence



intensity of **TBB** was barely changed in different pH value (3–10), suggesting that sensor **TBB** was greatly stable for pH value (Fig. S7). On treatment with  $\text{CN}^-$  ions, the fluorescence intensity was dramatically improved within the pH value from 5 to 9, thus **TBB** was able to detect  $\text{CN}^-$  ion in a broad pH range.

In order to evaluate the sensing selectivity of sensor **TBB** toward  $\text{CN}^-$  ion, the competitive experiments were performed with 100  $\mu\text{M}$  of various other anions ( $\text{H}_2\text{PO}_4^-$ ,  $\text{AcO}^-$ ,  $\text{F}^-$ ,  $\text{Cl}^-$ ,  $\text{Br}^-$ ,  $\text{I}^-$ ,  $\text{N}_3^-$ ,  $\text{NO}_3^-$ ,  $\text{SO}_4^-$  and  $\text{SCN}^-$ ) as well as 100  $\mu\text{M}$  of  $\text{CN}^-$  in THF– $\text{H}_2\text{O}$  (2:8, v/v) mixed solution of **TBB** (10  $\mu\text{M}$ ) (Fig. 6). The competitive anions barely improved the fluorescence intensity of **TBB** aqueous solution. Upon the addition of  $\text{CN}^-$  ion to the solution containing **TBB** and other anions, the fluorescence intensity was remarkably enhanced, which was almost similar to when other competitive anions were absent (Fig. 6). Therefore, the other anions were negligibly interfered the fluorescence response of **TBB** toward  $\text{CN}^-$  ion. The above results implied that sensor **TBB** was capable of sensing  $\text{CN}^-$  ion in aqueous solutions even with other competitive anions.

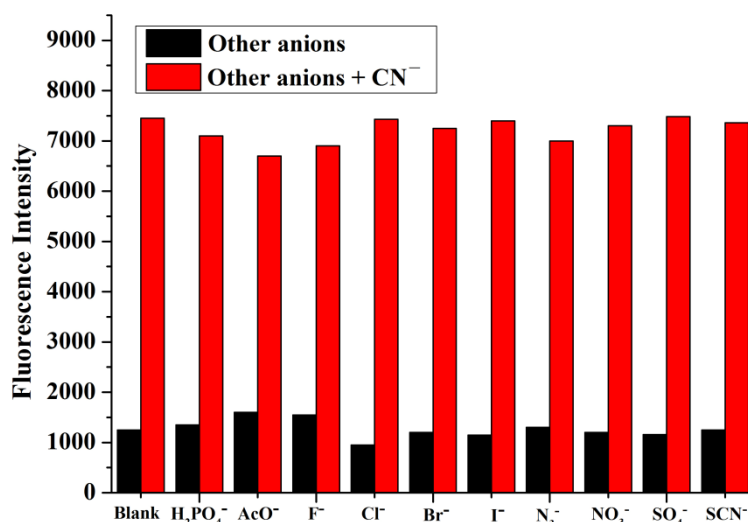


**Fig. 6.** The Histogram about the fluorescence intensity of sensor **TBB** (10 μM) in THF-H<sub>2</sub>O (2:8, v/v) mixed solution with 100 μM other anions (H<sub>2</sub>PO<sub>4</sub><sup>-</sup>, AcO<sup>-</sup>, F<sup>-</sup>, Cl<sup>-</sup>, Br<sup>-</sup>, I<sup>-</sup>, N<sub>3</sub><sup>-</sup>, NO<sub>3</sub><sup>-</sup>, SO<sub>4</sub><sup>-</sup> and SCN<sup>-</sup>) that before and after treating with CN<sup>-</sup> (100 μM), excited at 450 nm. The solutions were stirred for 3 min at 32 °C before the measurements.

### 3.5. The sensing mechanism

When the reaction of sensor **TBB** with CN<sup>-</sup> ion was performed at a high concentration in THF-H<sub>2</sub>O mixture, some light yellow precipitate was generated. After the simple purification, the precipitate structure was analyzed by the MS spectrometry, <sup>1</sup>H NMR and <sup>13</sup>C NMR spectra. As illustrated in Fig. S8, a peak at m/z 670.26 corresponding to the additive product [**TBB-CN** + H]<sup>+</sup> (cal. 670.21) was observed. In the <sup>1</sup>H NMR spectra of **TBB**, the peaks at 8.47 and 8.17 ppm were identified as the vinylic proton H<sub>1</sub> and H<sub>2</sub> that showed the large coupling constants [23], which up-field shifted to 5.76 and 4.97 ppm in product **TBB-CN**. Besides this, proton signals of the methyl group attached with N (H<sub>3</sub>) also displayed the up field shift from 5.35 to 3.61 ppm (Fig. 7). Moreover, the

signals appearing at 171.93 and 52.57 ppm in the  $^{13}\text{C}$  NMR spectrum of **TBB** corresponded to the carbons  $\text{C}_1$  and  $\text{C}_2$  respectively. While in product **TBB-CN**, these two peaks up-field shifted to 72.36 and 43.65 ppm, accompany with the presence of a new peak at 114.93 ppm, which was considered to be the carbon atom of cyano group [10]. The above results clearly illustrated that the nucleophilic addition of  $\text{CN}^-$  ion on the benzothiazolium  $\text{C}=\text{N}$  bond of **TBB** yielded the additive species **TBB-CN**. Unlike **TBB**, the film of **TBB-CN** on the glass plate exhibited an intense emission (Fig S9). Moreover, species **TBB-CN** displayed the different aggregation behavior from sensor **TBB**. The DLS data indicated the aggregation of **TBB-CN** (10  $\mu\text{M}$ ) in THF- $\text{H}_2\text{O}$  (2:8, v/v) mixed solution with the average particle size of 293.2 nm (Fig S10), whereas **TBB** (10  $\mu\text{M}$ ) was only able to aggregate in THF- $\text{H}_2\text{O}$  (1:99, v/v) mixture. Finally, the solution of **TBB-CN** exhibited an intense emission at 589 nm, which was similar with the solution of **TBB** in THF- $\text{H}_2\text{O}$  (2:8, v/v) mixture with  $\text{CN}^-$  ion (Fig S11). Therefore, the nucleophilic addition reaction of  $\text{CN}^-$  ion with sensor **TBB** in THF- $\text{H}_2\text{O}$  mixture produced the compound **TBB-CN**, whose aggregation gave rise to the intense emission (Scheme 2).

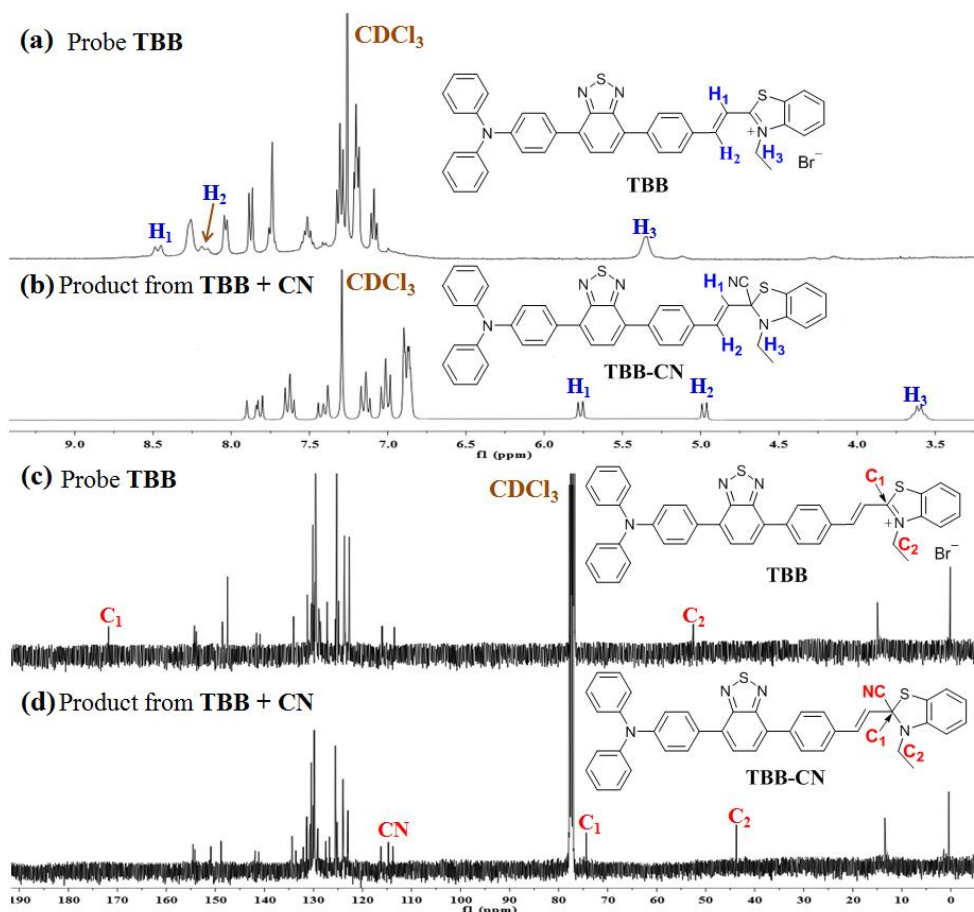
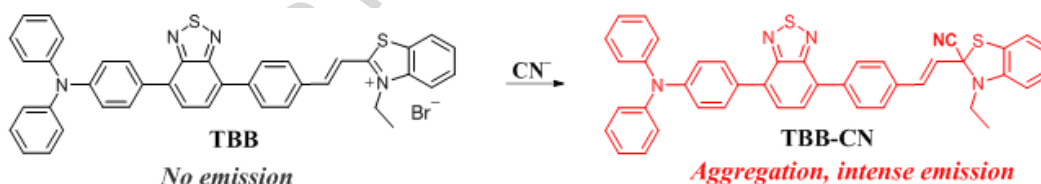


**Fig. 7.** The  $^1\text{H}$  NMR spectra of sensor **TBB** (a) and the product from the reaction of **TBB** with  $\text{CN}^-$  (b); The  $^{13}\text{C}$  NMR spectra of sensor **TBB** (c) and the product from the reaction of **TBB** with  $\text{CN}^-$  (d). The NMR spectra were tested in  $\text{CDCl}_3$ .



**Scheme 2.** The proposed sensing mechanism of sensor **TBB** toward  $\text{CN}^-$

### 3.6. The DFT studies

To better understand the fluorescence response of sensor **TBB** toward  $\text{CN}^-$  ion, the theoretical calculations were performed using the density functional theory (DFT) method with the TD-B3LYP level of the Gaussian 16 program. The frontier molecular orbitals and energy levels

of compounds **TBB** and **TBB-CN** were firstly revealed through time-dependent DFT (TDDFT) calculations, and the isovalue was set at 0.02 (Fig. 8). For **TBB**, the HOMO level was mainly localized on the TPA group, and LUMO level distributed on the acceptor moieties such as BT unit, the adjacent groups and benzothiazolium moiety, respectively. Such an orbital distribution implied that **TBB** had an extremely strong ICT tendency [31], which could quench the fluorescence in essence. Similarly with **TBB**, the HOMO level of **TBB-CN** also distributed on TPA group. But its LUMO level was primarily localized on the BT unit, because the nucleophilic addition of  $\text{CN}^-$  to benzothiazolium moiety destroyed its cationic structure and weakened the electron-withdrawing ability. In this case, **TBB-CN** had a larger HOMO-LUMO band gap (2.5652 eV) than **TBB** (2.1454 eV), thus its emission wavelength exhibited a blue-shift, which was consistent with the experimental results. In addition, the optional structure of **TBB-CN** in excited state was studied that using  $\text{H}_2\text{O}$  as the solvent molecule (Fig. S12). The BT unit and the adjacent benzene ring were almost coplanar, but the TPA group and the additive product of benzothiazolium with  $\text{CN}^-$  were highly twisted, which was responsible for the intense emission of **TBB-CN** in the aggregate state.

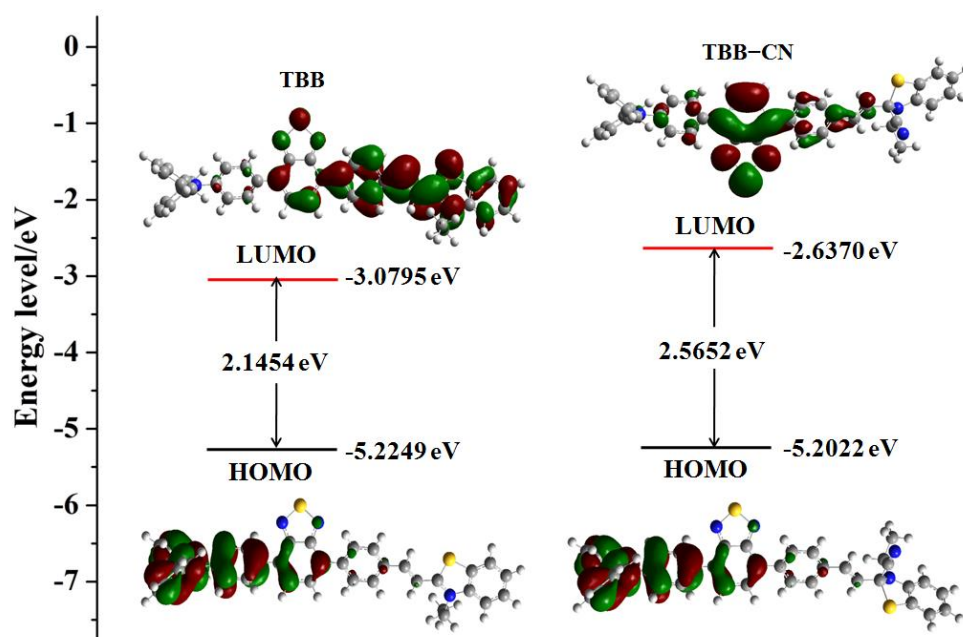


**Fig. 8.** Frontier molecular orbitals and the energy level diagram of **TBB** and **TBB-CN**. In the optional conformation, the yellow part represents the “S” atom, the blue part represents the “N” atom, the gray part represents the “C” atom and the white part represents the “H” atom.

#### 4. Conclusions

In summary, a novel colorimetric and fluorescence turn-on chemosensor **TBB** with benzothiazolium moiety for  $\text{CN}^-$  ion has been explored. Sensor **TBB** was scarcely emissive in THF/ $\text{H}_2\text{O}$  (2:8, v/v) mixture due to the strong intramolecular charge transfer (ICT) and dipole-dipole interaction. In the presence of  $\text{CN}^-$  ion, the nucleophilic addition of  $\text{CN}^-$  ion with benzothiazolium C=N bond of **TBB** produced the additive species **TBB-CN**, whose aggregation resulted in the intense orange-red emission. Meanwhile, the color of solution was visually changed from orange-yellow to light yellow. Sensor **TBB** exhibited the high selectivity to  $\text{CN}^-$  ion, and the sensing process

was completed within 3 min. Furthermore, the detection limit of 137 nM was far lower than the WHO guideline (1.9  $\mu$ M).

### Acknowledgments

This work was supported by the school foundation of Wuhan Textile University [grant number 183010]; and the young people fund of Hubei Education Department [grant number 184043].

### References

- [1] T.Z. Sadyrbaeva, Gold (III) recovery from non-toxic electrolytes using hybri-electrodialysis–electrolysis process, *Sep. Purif. Technol.* 86 (2012) 262–265.  
<https://www.sciencedirect.com/science/article/pii/S1383586611005971>.
- [2] D.T. Thompson, Cyanide: social, industrial and economic aspects, *Gold. Bull.* 34 (2001) 133–714. <https://doi.org/10.1007/BF03214826>.
- [3] D.W. Boening, C.M. Chew, A critical review: general toxicity and environmental fate of three aqueous cyanide ions and associated ligands, *Water. Air. Soil. Pollut.* 109 (1999) 67–79.  
<https://doi.org/10.1023/A:100500511>.
- [4] K.W. Kulig, B. Ballantyne, Cyanide toxicity, U.S. Department of Health and Human Services, 1991.  
<https://stacks.cdc.gov/view/cdc/7593>.
- [5] B. Vennesland, E.E. Comm, C.J. Knownles, J. Westly, F. Wissing, Cyanide in biology, Academic Press, London, 1981.  
<https://www.journals.uchicago.edu/doi/abs/10.1086/413208>.
- [6] Guidelines for drinking-water quality, fourth edition, World Health Organization, Switzerland, 2011.  
[https://www.who.int/water\\_sanitation\\_health/publications/2011/dwq\\_guidelines/en/](https://www.who.int/water_sanitation_health/publications/2011/dwq_guidelines/en/).

- [7] F. Wang, L. Wang, X. Chen, J. Yoon, Recent progress in the development of fluorometric and colorimetric chemosensors for detection of cyanide ions, *Chem. Soc. Rev.* 43 (2014) 4312-4324.  
<https://pubs.rsc.org/en/Content/ArticleLanding/2014/CS/c4cs00008k>.
- [8] D. Udhayakumari, Chromogenic and fluorogenic chemosensors for lethal cyanide ion, a comprehensive review of the year 2016, *Sensors Actuators B Chem.* 259 (2018) 1022-1057.  
<https://doi.org/10.1016/j.snb.2017.12.006>.
- [9] J. Li, X. Qi, W. Wei, Y. Liu, X. Xu, Q. Lin, W. Dong, A “donor-two-acceptor” sensor for cyanide detection in aqueous solution, *Sensors Actuators B Chem.* 220 (2015) 986–991.  
<https://doi.org/10.1016/j.snb.2015.06.042>.
- [10] I.J. Kim, M. Ramalingam, Y.A. Son, A reaction based colorimetric chemosensor for the detection of cyanide ion in aqueous solution, *Sensors Actuators B Chem.* 246 (2017) 319–326.  
<https://doi.org/10.1016/j.snb.2017.02.015>.
- [11] X. Yu, K. Wang, D. Cao, Q. Wu, R. Guan, Y. Xu, Y. Sun, Z. Liu, Simple benzothiazole chemosensor for detection of cyanide anions via nucleophilic addition, *Chem. Heterocycl. Comp.* 53 (2017) 42-45. <https://doi.org/10.1007/s10593-017-2019-7>.
- [12] W.N. Wu, H. Wu, Y. Wang, X.L. Zhao, Z.Q. Xu, Z.H. Xu, Y.C. Fan, A NIR sensor for cyanide detection and its application in cell imaging, *Spectrochim. Acta A* 199 (2018) 141–145.  
<https://doi.org/10.1016/j.saa.2018.03.044>.
- [13] D. Wu, A.C. Sedgwick, T. Gunnlaugsson, E.U. Akkaya, J. Yoon, T.D. James, Fluorescent chemosensors: the past, present and future, *Chem. Soc. Rev.* 46 (2017) 7105–7123.  
<https://pubs.rsc.org/en/content/articlelanding/2017/cs/c7cs00240h>.
- [14] J. Liang, B.Z. Tang, B. Liu, Specific light-up bioprobes based on



AIEgen conjugates, *Chem. Soc. Rev.* 44 (2015) 2798–2811.

<https://doi.org/10.1039/C4CS00444B>

[15] J. Li, W. Wei, X. Qi, G. Zuo, J. Fang, W. Dong, Highly selective colorimetric/fluorometric dual-channel sensor for cyanide based on ICT off in aqueous solution, *Sensors Actuators B Chem.* 228 (2016) 330–334. <https://doi.org/10.1016/j.snb.2016.01.055>.

[16] J. Li, X. Qi, W. Wei, G. Zuo, W. Dong, A red-emitting fluorescent and colorimetric dual-channel sensor for cyanide based on a hybrid naphthopyran-benzothiazol in aqueous solution, *Sensors Actuators B Chem.* 232 (2016) 666–672. <https://doi.org/10.1016/j.snb.2016.04.021>.

[17] N. Mergu, J.H. Moon, H. Kim, G. Heo, Y.-A. Son, Highly selective naphthalimide-benzothiazole hybrid-based colorimetric and turn on fluorescent chemosensor for cyanide and tryptophan detection in aqueous media, *Sensors Actuators B Chem.* 273 (2018) 143–152. <https://doi.org/10.1016/j.snb.2018.05.165>.

[18] J. Mei, N.L.C. Leung, R.T.K. Kwok, J.W.Y. Lam, B.Z. Tang, Aggregation-induced emission: together we shine, united we soar, *Chem. Rev.* 115 (2015) 11718–11940. <https://pubs.acs.org/ccindex.cn/doi/10.1021/acs.chemrev.5b00263>.

[19] M. Gao, B.Z. Tang, Fluorescent sensors based on aggregation-induced emission: recent advances and perspectives, *ACS Sens.* 2 (2017) 1382–1399. <https://pubs.acs.org/ccindex.cn/doi/10.1021/acssensors.7b00551>.

[20] J. Mei, Y. Huang, H. Tian, Progress and trends in AIE-based bioprobes: a brief overview, *ACS Appl. Mater. Interfaces.* 10 (2018) 12217–12261. <https://pubs.acs.org/ccindex.cn/doi/10.1021/acsami.7b14343>.

[21] Q. Zhao, J.Z. Sun, Red and near infrared emission materials with AIE characteristics, *J. Mater. Chem. C* 4 (2016) 10588–10609.

<https://pubs.rsc.org/en/content/articlelanding/2016/tc/c6tc03359h>.

[22] T. Ishi-I, Y. Taguri, S. Kato, M. Shigeiwa, H. Gorohmaru, S. Maeda, S. Mataka, Singlet oxygen generation by two-photon excitation of porphyrin derivatives having two-photon-absorbing benzothiadiazole chromophores, *J. Mater. Chem.* 17 (2007) 3341–3346.

<https://pubs.rsc.org/en/Content/ArticleLanding/2007/JM/b704499b>.

[23] N. Zhao, Z. Yang, J.W.Y. Lam, H.H.Y. Sung, N. Xie, S. Chen, H. Su, M. Gao, I.D. Williams, K.S. Wong, B.Z. Tang, Benzothiazolium-functionalized tetraphenylethene: an AIE luminogen with tunable solid-state emission, *Chem. Commun.* 48 (2012) 8637–8639.

<https://pubs.rsc.org/en/Content/ArticleLanding/CC/2012/C2CC33780k>.

[24] T. Sun, Q. Niu, Y. Li, T. Li, T. Hu, E. Wang, H. Liu, A novel oligothiophene-based colorimetric and fluorescent “turn on” sensor for highly selective and sensitive detection of cyanide in aqueous media and its practical applications in water and food samples, *Sensors Actuators B Chem.* 258 (2018) 64–71.

<https://doi.org/10.1016/j.snb.2017.11.095>.

[25] R. Hu, E. Lager, A. Aguilar-Aguilar, J. Liu, J.W.Y. Lam, H.H.Y. Sung, I.D. Williams, Y. Zhong, K.S. Wong, E. Penã-Cabrera, B.Z. Tang, Twisted intramolecular charge transfer and aggregation-induced emission of BODIPY derivatives, *J. Phys. Chem. C* 113 (2009) 15845–15853.

<https://pubs.acs.org/ccindex.cn/doi/abs/10.1021/jp902962h>.

[26] C. Gao, M.K. Hossain, M.A. Wahab, J. Xiong, B.M. Qiu, H. Luo, W. Li, Understanding the details of aggregation-induced emission (AIE) effect in D- $\pi$ -A type imidazolium-based compounds through the stepwise change of rotatable moieties. *Dyes Pigments* 160 (2019) 909-914.

<https://doi.org/10.1016/j.dyepig.2018.08.032>.

[27] Q. Zhang, Y. Li, H. Zuo, C. Wang, Y. Shen, A new colorimetric and ratiometric chemodosimeter for mercury (II) based on triphenylamine and

benzothiadiazolenovel, J. Photochem. Photobio. A 332 (2017) 293–298.

<https://doi.org/10.1016/j.jphotochem.2016.09.007>.

[28] C. Gao, M.K. Hossain, L. Li, M.A. Wahab, J. Xiong, W. Li, A colorimetric and fluorescence turn-on chemosensor for the highly selective detection of hydrogen peroxide in aqueous solution, J. Photochem. Photobio. A 368 (2019) 97–103.

<https://doi.org/10.1016/j.jphotochem.2018.09.020>.

[29] Y. Hong, J.W.Y. Lam, B.Z. Tang, Aggregation-induced emission: phenomenon, mechanism and applications, Chem. Commun. 0 (2009) 4332-4353.

<https://pubs.rsc.org/en/content/articlelanding/2009/cc/b904665h>.

[30] R. Wang, M. Hou, Z. Xu, L. Tan, C. Zhong, L. Zhu, A new red fluorophore with aggregation enhanced emission by an unexpected “one-step” protocol, RSC Adv. 8 (2018) 18327–18333.

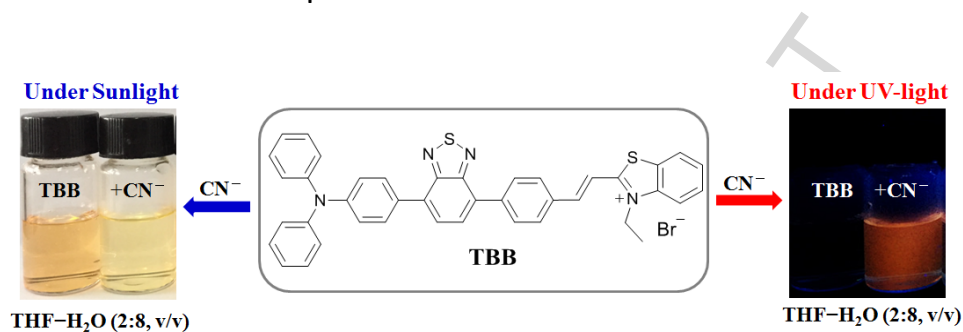
<https://pubs.rsc.org/en/content/articlelanding/2018/ra/c8ra00955d>.

[31] X.Y. Shen, Y.J. Wang, E. Zhao, W.Z. Yuan, Y. Liu, P. Lu, A. Qin, Y. Ma, J.Z. Sun, B.Z. Tang, Effects of substitution with donor–acceptor groups on the properties of tetraphenylethene trimer: aggregation-induced emission, solvatochromism, and mechanochromism, J. Phys. Chem. C 117 (2013) 7334–7347.

<http://pubs.acs.org/doi/abs/10.1021/jp311360p>.

**Graphical abstract:**

A novel colorimetric and fluorescence turn-on sensor **TBB** with benzothiazolium moiety for cyanide ion ( $\text{CN}^-$ ) detection in THF– $\text{H}_2\text{O}$  (2:8, v/v) mixture has been explored.



## Highlights

- A novel chemosensor **TBB** with benzothiazolium moiety for  $\text{CN}^-$  ion has been explored.
- Sensor **TBB** exhibits the high selectivity to  $\text{CN}^-$  ion in aqueous solution.
- The presence of  $\text{CN}^-$  ion results in the color change and fluorescence turn-on.
- The sensing mechanism is verified by NMR, MS spectrometry and DFT calculations.